Schwanen *et al.*
Environmental Sciences Europe (2023) 35:15
https://doi.org/10.1186/s12302-023-00717-4

Environmental Sciences Europe

RESEARCH

Open Access

Distribution, remobilization and accumulation of organic contaminants by flood events in a meso-scaled catchment system

Christina A. Schwanen[1], Jan Müller[1], Philipp Schulte[2] and Jan Schwarzbauer[1*]

Abstract

Background Extreme weather events and natural disasters such as floods can cause severe damage and impacts on catchment systems covering natural as well as urban, industrial or agricultural areas. Thus, floods often lead to the acute and unusual release of organic pollutants, as well as the remobilization of legacy contaminations or old burdens. Floodplains are then of major relevance for the accumulation of pollutants. Accordingly, various floodplains distributed throughout the course of the Rur River were sampled immediately after two flood events in January/February and July 2021. The main objective was to address the general lack of knowledge on indirect effects of flooding and the corresponding distribution and accumulation of organic pollutants regarding different dimensions and dynamics of flood events.

Results Gas Chromatography/Mass Spectrometry (GC/MS) based non-target screenings revealed the presence of several lipophilic to moderate polar organic pollutant groups, including PAHs (polycyclic aromatic hydrocarbons), hopanes, PCBs (polychlorinated biphenyls), LABs (linear alkylbenzenes) and various other industrial substances. These substances are indicators of petrogenic pollution, historical and current industry in the catchment area, and of wastewater and urban pollution, respectively. In general, concentrations detected after the extreme summer flood were higher than in winter. This points to additional emission sources due to substantially higher discharges and consequently more severe flooding in July. The main tributaries also had a major influence on the input and concentrations of organic pollutants at the receiving Rur River. Further on, structural features such as dams and reservoirs, but also (re)naturalized areas were clearly recognizable in the flood-related dispersion of organic pollutants. Interestingly, LAB contamination was similar after both flood events regardless of the specific dimension.

Conclusions Flood dimension and frequency are of great relevance for the distribution, remobilization and accumulation of organic contaminants. However, special attention should be given to the introduction of wastewater pollutants for any flood extent. Overall, organic indicators are therefore very useful to obtain information on specific distribution patterns and the influence of tributaries or structural measures, providing an important basis for the assessment of short- and long-term environmental risks and hazards.

Keywords Flood events, Organic pollution, Remobilization, Vulnerability, Hazard

*Correspondence:
Jan Schwarzbauer
jan.schwarzbauer@emr.rwth-aachen.de
[1] Institute of Geology and Geochemistry of Petroleum and Coal, RWTH Aachen University, Lochnerstraße 4-20, 52056 Aachen, Germany
[2] Department of Geography, RWTH Aachen University, Templergraben 55, 52056 Aachen, Germany

Background

In recent years, the number of extreme weather events and natural disasters has increased worldwide, which has also led to an increase in flooding. To mention just a few recent examples, in the twenty-first century major floods occurred on European rivers in 2002, 2005, 2007, 2010 and 2013 [26, 34]. Due to global climate change, severe flood events like these are likely to occur more frequently and also with higher intensities in the coming decades (e.g., [20, 26, 60]). In addition to infrastructural and economic damage, flood events have a direct and indirect impact on humans, animals and the environment. It is particularly important to consider the ecological damage due to the discharge of pollutants and toxic substances into river systems by a flooding of industrial sites, landfills, agricultural areas as well as urban areas including wastewater treatment plants. The resulting release of substances leads to an increased environmental contamination and can affect formerly unpolluted sites. In return, in many catchments, there is also a risk that contaminated sediments and old burdens will be remobilized during floods [8]. In particular, this effect has been scarcely studied to date.

Generally, different inorganic and organic substances tend to be enriched in sediments due to their mainly hydrophobic and lipophilic character. These substances include heavy metals and a variety of organic contaminants such as PAHs, LABs, PCBs or pesticides. In particular, the input and distribution of metals and PAHs have been intensively studied in flood deposits (e.g., [30, 31, 53]). Nevertheless, there are several further pollutants that need to be investigated to assess risks for human health and environmental protection. These include substances that are generally difficult to be degraded in wastewater treatment plants or the aquatic environment. In addition, substances of high production or emission rates but principally degradable also enter water bodies and possess therefore also environmental relevance. This can locally result in a cumulative contamination potentially posing a significant risk to environmental quality as well as human and animal health [8].

Especially floodplains are an important sink for sedimentary material and accumulated pollutants. Their natural functions include aspects such as water, sediment and nutrient retention, flood protection, groundwater recharge as well as the self-purification of water bodies. However, nowadays people use these areas for various other purposes such as agriculture, settlement or infrastructure (e.g., for the construction of rail- or motorways). Due to these impacts and associated large losses of floodplains in the past, only about one-third of the former floodplain areas on rivers in Germany can still be inundated during large flood events [24]. Nevertheless, the existing floodplains are important accumulation areas for particulate matter and organic contaminants as POPs (persistent organic pollutants), which is why they are also referred as the river's memory of contamination [18, 23].

Due to extreme precipitation and runoff during the period 12 to 15 July 2021, severe flooding occurred in Germany and other neighboring countries [25, 47]. Within a very short period of time, an extreme amount of precipitation fell over the low mountain ranges in Rhineland-Palatinate and North Rhine-Westphalia in Germany. This amount was partly more than twice as high as the average for the entire month of July [21, 36]. Furthermore, the soils were saturated by previous rain events and therefore could not absorb the water masses [6, 25]. Particularly in low mountain ranges such as the Eifel, this led to rapid rises in water levels as the water was channelled and collected in the river courses. Overall, the severe weather event and flooding had extreme impacts in terms of great damage to infrastructure (including houses, roads, rail- and motorway lines, bridges and communication), but also in terms of more than 200 fatalities [6, 25, 47]. In addition to these direct impacts, it is also important to study longer-term or indirect impacts such as the input and accumulation of pollutants in river systems.

Therefore, different floodplains distributed throughout the course of the Rur River were sampled immediately after two flood events in January/February and July 2021. The main objectives were to determine pollutant concentrations, (re)distribution, and accumulation, as well as to understand the dimension and corresponding impacts of different floods on a meso-scaled catchment system. This was all done under the framework of risk assessment and pollutant mitigation during and after flood events.

Methods

Study area and sampling

The 163-km-long Rur river runs from the High Fens in Belgium through the typical low-mountain range landscape of the Eifel to the lowland part of the Lower Rhine Embayment in western Germany to its confluence with the Meuse in Roermond (Netherlands) [46]. The catchment covers various land uses and has natural river sections, immediate urban settlement, several industries (e.g., paper processing) and agriculture. Furthermore, the region is historically characterized by centuries of underground mining and nowadays by lignite mining. Overall, there are more than 40 wastewater treatment plants (WWTPs) in the Rur catchment area, mostly located in the lower parts and the corresponding tributaries

(especially Inde and Wurm). Together with the tributary Urft, Inde and Wurm are also the most relevant tributaries in terms of discharge.

Sediment samples were taken on July 22, 2021, as well as on February 5, 2021, shortly after corresponding flood events in July, respectively, January/February. In detail, samples were taken at 16 (July), respectively, 13 sites (February) throughout the entire course of the river (Fig. 1). Sampling was done after the flood had subsided at the floodplains and prior to the next rain event. Hence, the material was not subject to any washing out or relocation. The material was taken near the surface (at a depth of 0 to 3 cm) as a composite sample from an area of about 1 m^2 at the respective floodplain. The samples with a total weight of 200 to 300 g were stored in solvent-cleaned glass flasks at 4 °C in the dark

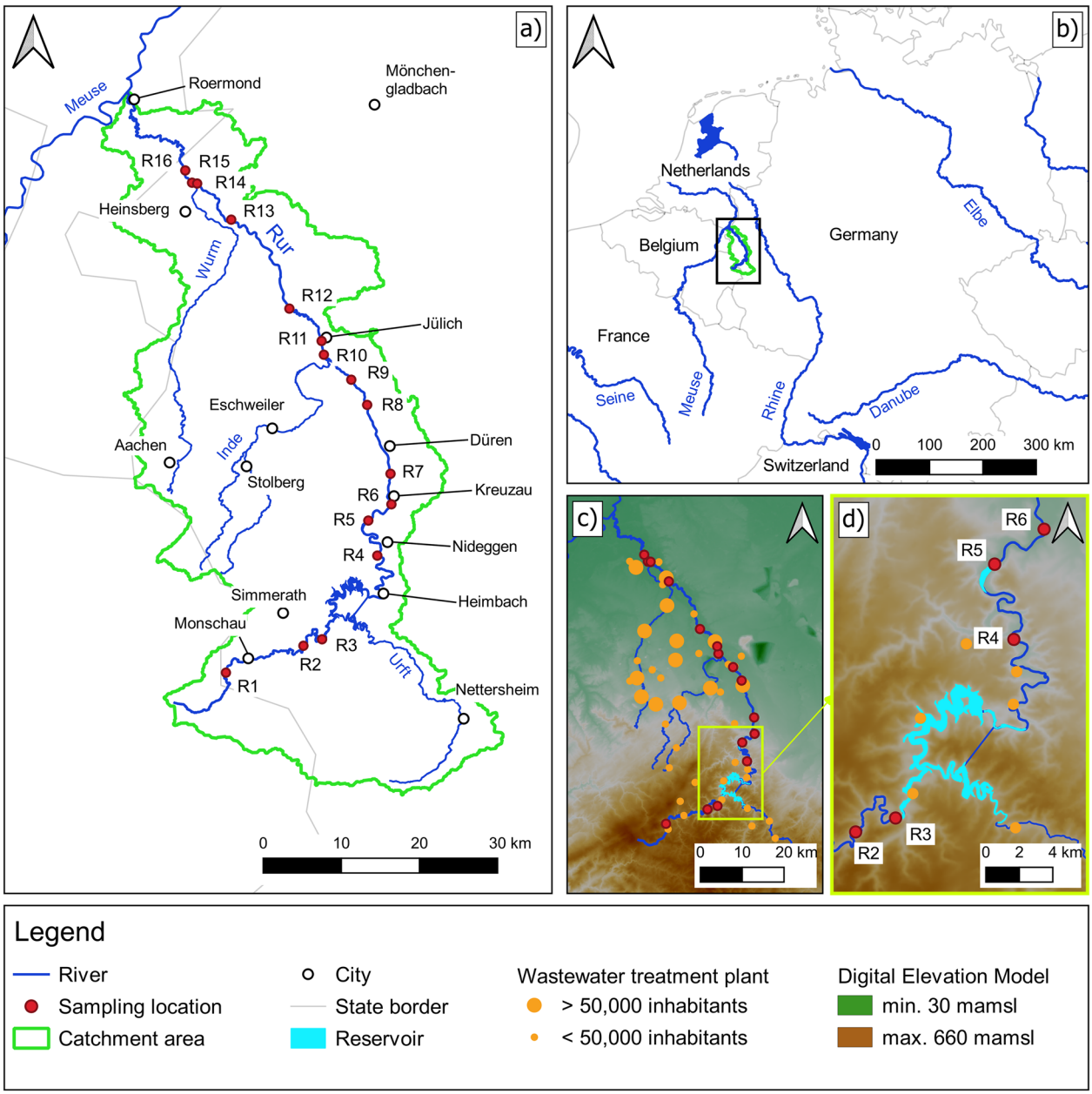

Fig. 1 Overview of the Rur catchment. **a** Rur catchment with sampling locations and important tributaries, **b** location of the Rur catchment in an European context, **c** wastewater treatment plants and elevations (meters above mean sea level, mamsl), **d** reservoirs in the upper course of the Rur

prior to analysis. Besides organic geochemical analysis, all samples were also analyzed for grain size and total organic carbon (TOC).

Standard parameters

Grain sizes were determined using a Beckman Coulter LS 13 320 laser diffraction particle size analyzer (Beckman Coulter GmbH, Krefeld, Germany) on the fraction < 2 mm. Sediments were treated with 30% H_2O_2 to remove organic matter and with 1.25 mL $Na_4P_2O_7$ in an overhead shaker for 12 h to prevent particle agglutination [33]. According to Schulte et al. [39], the device was equipped with an aqueous liquid module and a Polarization Intensity Differential Scatter unit. The grain size distribution was calculated using the Mie theory (Fluid RI: 1.33; Sample RI: 1.55; Imaginary RI: 0.1; cf [38]). and is given as percentage size frequency of 116 classes within a size range of 0.04–2000 µm. Furthermore, the content of total organic carbon (TOC), total carbon (TC) and total inorganic carbon (TIC) of each sample was determined by loss on ignition (LOI) using the liquiTOC II (Elementar Analysensysteme GmbH, Langenselbold, Germany). Dried sample aliquots of 0.1 g were heated and ashed at 550 °C (TOC) and 1000 °C (TIC) and the following difference in mass was used to calculate the (in)organic content. Finally, TOC concentrations were used to normalize the concentration of organic compounds to allow a comparability between different samples and sampling campaigns.

Organic geochemical analysis

Sample extraction

Aliquots of around 20 g of untreated sediment were extracted using accelerated solvent extraction (Dionex ASE 150, Thermo Fisher Scientific, Waltham, MA, USA). Samples were extracted sequentially with approximately 30 mL of acetone, acetone/*n*-hexane 1:1 (v/v) and *n*-hexane. During each extraction step, the extraction cell was held at a temperature of 100 °C and a pressure of 10 MPa for a period of 5 min for static extraction. After each step, the extracts were collected and combined. Following the separation and disposal of the aqueous phase, the sample extract was concentrated to a volume of 5 mL by rotary evaporation and then dried with anhydrous granulated sodium sulphate (Na_2SO_4). Again, the extract was concentrated to a volume of 0.5 mL and activated copper powder was added to remove elemental sulphur when ultrasonically treated for 15 min.

Fractionation

According to the polarity of the organic contaminants, the extract was separated into six fractions by column chromatography. Columns were filled with 2 g activated silica gel and conditioned over night at 200 °C. Mixtures of *n*-pentane, dichloromethane and methanol were used as eluents with increasing polarity [42]:

- Fraction B1: 5 mL *n*-pentane,
- Fraction B2: 8.5 mL *n*-pentane/DCM 95/5,
- Fraction B3: 5 mL *n*-pentane/DCM 90/10,
- Fraction B4: 5 mL *n*-pentane/DCM 40/60,
- Fraction B5: 5 mL DCM,
- Fraction B6: 5 mL methanol.

The acidic compounds in the sixth fraction (B6) were methylated by adding Bf_3-methanol. The resulting extract was then evaporated and fractionated by column chromatography into two further subfractions using 3 mL of *n*-pentane/DCM 40/60 plus 6 mL of DCM (fraction B6K1) and 5 mL of methanol as eluents (B6K2). An internal standard (5.8 ng/µL fluoroacetophenone, 6.3 ng/µL d_{10}-benzophenone and 6.0 ng/µL d_{34}-hexadecane) was added to fractions B1 to B5 (50 µL) as well as fraction B6K1 (200 µL). Prior to injection, all fractions were concentrated to final volumes of 50 to 200 µL (fractions B1 to B5) and 200 to 800 µL (fractions B6).

Gas chromatography–mass spectrometry analyses

GC/MS analyses were performed on a quadrupole ThermoQuest Trace MS mass spectrometer linked to a ThermoQuest Trace GC equipped with a ZB-5 fused silica capillary column (Phenomenex, Aschaffenburg, Germany; 30 m × 0.25 mm ID × 0.25 µm film thickness). Carrier gas flow was 1.5 mL/min. For all fractions, a 1 µL split/splitless injection (injector temperature of 270 °C) was carried out at 60 °C with a splitless time of 60 s, 3 min hold, then programmed at 3 °C/min to 310 °C with 20 min isothermal time. Operation took place in full-scan mode (EI^+, 70 eV) using a source temperature of 200 °C, scanning from 35 to 700 amu at a rate of 1.5 scans/s.

Compound identification and quantification

Organic compounds were identified by comparison with mass spectral databases (NIST, Wiley) and published information. Verification was achieved by comparison of specific gas chromatographic and mass spectral parameters (e.g., retention times and elution orders) with those of purchased reference material. Quantification was based on peak integration of characteristic

ion chromatograms and an external four-point calibration with reference material. A surrogate standard was used to correct inaccuracies of injection and sample volume. The detection limit was in the range of 1 ng/g_{TOC} (calculated based on signal-to-noise ratios in real sample matrix) and therefore, no attempts were made to quantify concentrations lower than 5 ng/g_{TOC}. Recovery rates for the analytes in this study ranged between 70 and 100 % (with exception of naphthalene and DIPNs with values around 50 %). Blank analyses (n=2) were done to identify possible background and laboratory contaminations and revealed neglectable concentrations of a few PAHs, DIPNs and BHT.

Results

Since the TOC content plays a major role in pollutant distribution and accumulation, all concentration values were normalized to the TOC content for better comparability between different locations as well as campaigns. The TOC content varied between 0.2 and 7.6% in July and 0.7 and 6.8% in February 2021. The highest TOC levels occurred in the middle course of the Rur in both campaigns. A similar pattern was also found for the grain size distribution with the finest samples in the middle course. The samples from the Eifel region were mainly very coarse sands and in the lower reaches silty medium to coarse-grained sands were present.

GC/MS-based non-target screenings revealed the presence of a wide spectrum of organic compounds covering different groups of organic pollutants (cf. Table 1). Particularly, petrogenic contaminants such as polycyclic aromatic hydrocarbons (PAHs) and geohopanes were identified, but also various compounds attributable to urban (e.g., LABs) and industrial emission sources (e.g., DPE, DIPNs, PCBs).

Table 1 Maximum concentrations [µg/g_{TOC}] and corresponding sampling locations of different pollutants/pollutant groups

Pollutant (group)	Maximum concentration [µg/g_{TOC}]	
	February	July
LABs	6.9 (R15)	4.4 (R15)
PAHs (EPA16)	247 (R4, R12)	500 (R2)
Hopanes	0.4 (R3)	11.5 (R15)
PCBs		
6 congeners	6.1 (R12)	13.7 (R6)
Total	30.7 (R12)	68.8 (R6)
DIPN	4.1 (R12)	14.2 (R9)
DPE	0.01 (R2)	0.8 (R15)
Mesamoll®	0.75 (R8)	1.3 (R6)
BHT	< 0.005 (R2)	2.3 (R11)
N-Benzylformamide	< 0.005 (R11)	0.05 (R15)
Methyltriclosan	0.02 (R16)	0.08 (R14)

Many of the identified compounds were PAHs with concentrations up to 103 µg/g_{TOC} in July and up to 50.2 µg/g_{TOC} in February. ΣEPA16 PAH exposure occurred mainly in the high µg/g_{TOC} range (July: 69 to 500 µg/g_{TOC}; February: 31 to 247 µg/g_{TOC}). Further identified substances were so-called hetero-PAHs, which have one or more heteroatom (N, S, O) in their aromatic moieties. As a result, they exhibit increased water solubility compared to the generally lipophilic PAHs. They occurred with concentrations up to 32.4 µg/g_{TOC} in July and up to 4.5 µg/g_{TOC} in February. Overall, PAHs are common environmental pollutants and identified in several studies regarding environmental and flood pollution (e.g., [27, 30, 53]). They can originate from fossil fuels (e.g., due to seepage or oil spills) or be a result of incomplete combustion processes of organic matter. Therefore, PAHs also occur naturally and do not necessarily indicate anthropogenic input, but, nevertheless, they show a high biological and chemical stability in the environment and many PAHs are carcinogenic, mutagenic or toxic for reproduction [1, 17].

Geohopanes as diagenetic products of biohopanes can additionally indicate petrogenic contaminations and thus anthropogenic or urban emissions (e.g., from oil heating systems or vehicles). For instance, the ratio $T_s/(T_s+T_m)$ and the quantitative distribution of (22S)- and (22R)-homohopanes can indicate thermally mature organic material introduced into the river system by contamination from, e.g., fossil fuels [11, 15, 62]. The homologous series of C_{29}- to C_{35}-hopane stereoisomers was detected with total concentrations up to 11.5 µg/g_{TOC} in July and 0.4 µg/g_{TOC} in February.

Linear alkylbenzenes (LABs) are alkylated benzenes with linear C_{10} to C_{13} alkyl chains (phenyldecanes, phenylundecanes, phenyldodecanes and phenyltridecanes). They were identified in the samples of the Rur floodplains with maximum concentrations of 4.4 µg/g_{TOC} in July and 6.9 µg/g_{TOC} in February. LABs are common detergent residues with an enhanced lipophilicity and environmental stability and can therefore be used as anthropogenic markers of wastewater pollution. Furthermore, the abundance of specific LAB isomers or systematic changes in their composition can be used as indicator to determine the degree of (microbial) degradation [49].

Another well-known group of pollutants are polychlorinated biphenyls (PCBs). PCBs are man-made and thus, artificial and were once widely used in industrial applications as for instance in electrical insulation or hydraulic equipment [54, 55]. Manufacturing and usage of PCBs is banned for more than 30 years, but they are still

ubiquitously distributed in the aquatic environment as they have a high persistence and are not easily degradable. As a consequence of their lipophilicity and low vapor pressure, PCBs have a tendency to accumulate in soils, sediments and also in biota [41, 55]. However, they are carcinogenic to humans and have further adverse effects in terms of endocrine disruption and neurotoxicity. Representative congeners as PCB 28 (Cl_3-PCB), PCB 52 (Cl_4-PCB), PCB 101 (Cl_5-PCB), PCB 138 (Cl_6-PCB), PCB 153 (Cl_6-PCB) and PCB 180 (Cl_7-PCB) were detected with maximum concentrations up to 4.7 µg/g_{TOC} in July and 2.1 µg/g_{TOC} in February. To quantify the total PCB contamination, the sum of the representative PCBs has been multiplied by 5. As recommended by the German Environment Agency (UBA), this value reflects their constant relative proportion. Consequently, the total contamination was estimated to be maximum 68.8 µg/g_{TOC} in July and 30.7 µg/g_{TOC} in February.

Furthermore, different compounds suggesting an industrial origin were detected in the floodplains such as alkylsulfonic acid phenyl esters (Mesamoll®), di-*iso*-propylnaphthalenes (DIPNs) or 1,2-diphenoxyethane (DPE). Mesamoll® is a mixture of various alkylsulfonic acid phenyl esters that is used as an alternative for phthalate-based plasticizers. Its ability to sorb to sedimentary material indicates a wide distribution in the environment [14]. As a second relevant group, DIPNs are highly persistent and bioaccumulative and have several industrial applications (e.g., as PCB substitutes). Among others, they are used as technical agents to produce specialty papers and have therefore also been detected in recovered papers and packaging made from recycled paper [7, 12]. Further on, DPE is a characteristic compound of wastewaters from modern paper production sites, and both were already found in the water of the Rur river [40]. For the investigated floodplains, the maximum concentrations for Mesamoll® were 1.3 µg/g_{TOC} in July and 0.75 µg/g_{TOC} in February, for DIPN 14.2 µg/g_{TOC} in July and 4.1 µg/g_{TOC} in February and for DPE 800 ng/g_{TOC} in July and 13 ng/g_{TOC} in February.

Discussion

To understand the levels of pollution, to identify possible emission sources and to determine specific environmental behaviors of organic contaminants as the result of floods, the concentration trends were assessed over the entire river course (see Fig. 2). A special focus is placed on different dimensions and dynamics of the respective flood events and the varying extent of the impacts. This will also include an assessment to which degree remobilization and further relocation of the pollutants has taken place.

Both flood events differ in particular in water level and discharge. The normal mean water level at Jülich (close to R11), at the transition from the middle to the lower course of the Rur river, is 1.24 m and the average discharge of the Rur is 16.2 m^3/s [10, 45]. The winter flood had a maximum water level of 2.43 m and a maximum daily mean value of 73.2 m^3/s, while the summer flood at the same location even caused a water level over 4 m and a maximum discharge of 207 m^3/s [10, 45, 58]. The values in January did not exceed flood events with an annularity of 5 years and can therefore be considered as a regular event. However, the discharge in July was high above the previous measured maximum discharge of 173 m^3/s

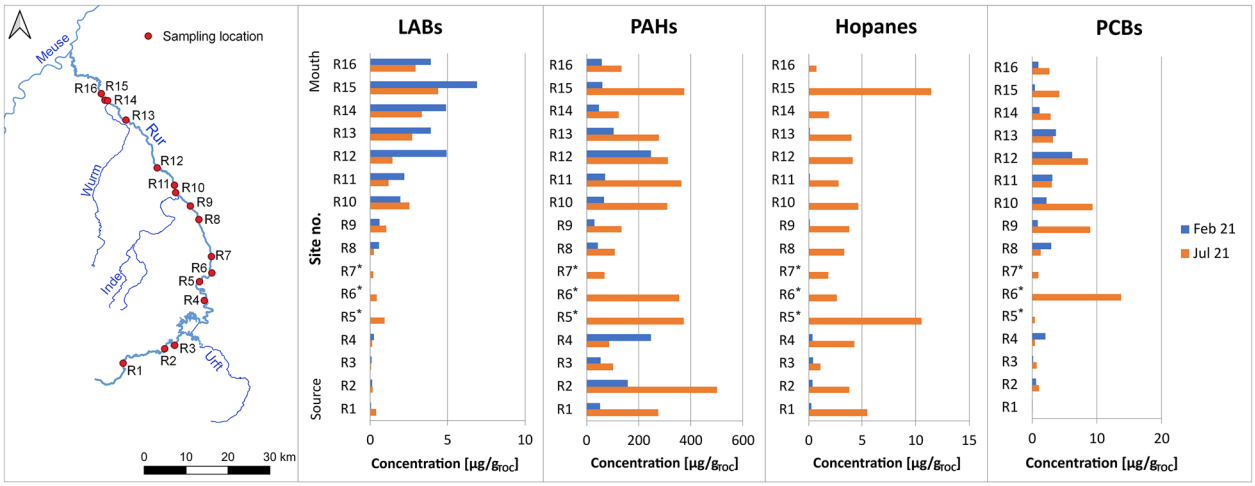

Fig. 2 Spatial distribution of LABs, PAHs, hopanes and PCBs over the Rur River course. Samples have been taken after two flood events in January/February and July 2021. (*) R5 to R7 were not sampled in February

in 1947 indicating the extreme dimension of this flood event [10].

Wolf et al. [61] have shown that the concentrations of suspended sediment in the Rur River are increased with higher discharge. They have been especially high due to the extreme flood event in summer. As the dispersion of lipophilic to semi-polar organic pollutants is strongly dependent on sediment transportation, an increased environmental contamination after the flood is assumed. This effect and the different flood dimensions are reflected in the measured concentrations of various substances. In general, concentrations detected after the July flood were mainly higher than in February. However, for some substances no considerable differences in concentrations occurred between both flood events (cf. Fig. 2). These differences and possible causes are discussed in more detail in following. Particular attention will be paid to tributary inflows and structural features of the river system, as these can also play a significant role in flood events.

Compounds with no considerable differences in concentrations

Specific pollutants that are quantitatively not affected by the different intensities of both flood events are LABs. They are indicative for domestic wastewater and, as shown in Fig. 3, occurred at high concentrations in the Rur floodplains downstream of Düren (R8). The city of Düren is the first big agglomeration with the largest WWTP in the catchment that is discharging its effluents directly into the Rur. In general, the largest WWTPs are located in the lower reaches of the Rur including its northern tributaries. This is well reflected in the concentration profiles of LABs determined in this study. For both flood events, the concentrations showed a clear increase downstream, which matches well with urban and industrial settlements. Particularly, the Inde and Wurm tributaries were clearly evident in the LAB emission patterns (R10 and R15). Several large WWTPs located on both tributaries consistently represent emission sources for LABs and thus explain the steady inputs. In fact, the highest overall concentrations occurred after

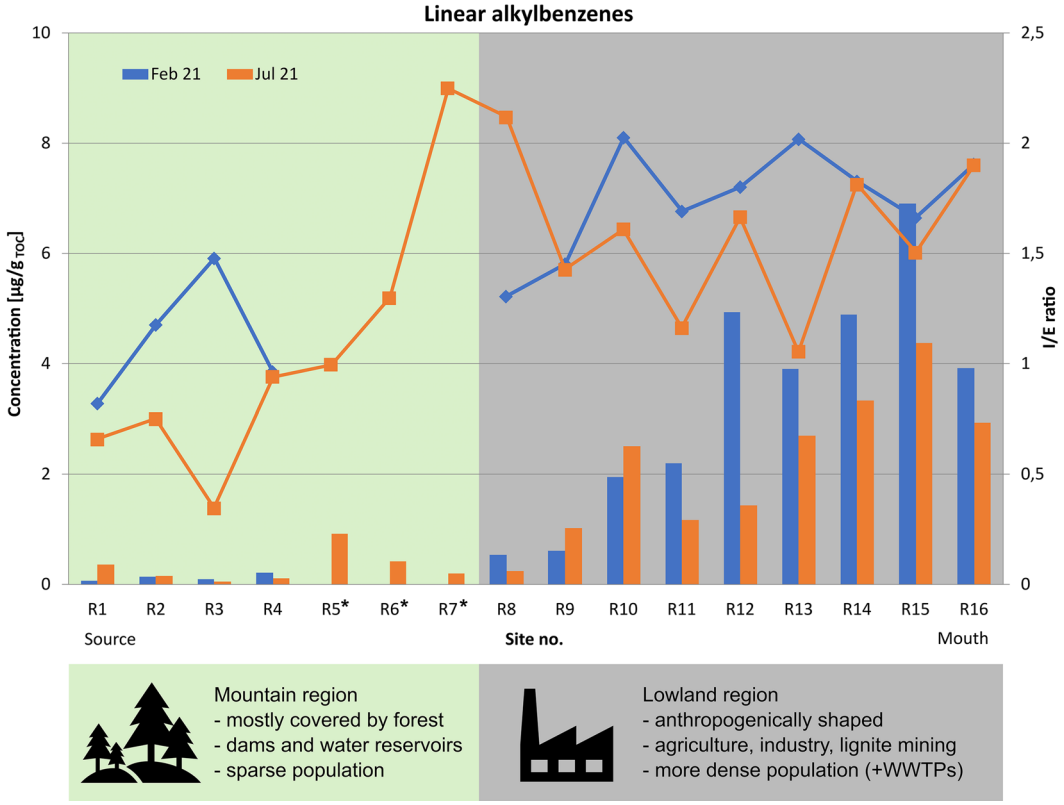

Fig. 3 Spatial distribution of LAB concentrations and I/E ratios [µg/g_{TOC}] over the Rur River course. I/E ratios close to 0.7 represent untreated wastewater, while higher values represent ongoing microbial degradation according to Takada and Eganhouse [48]. (*) R5 to R7 were not sampled in February

the Wurm tributary inflow (Feb.: 6.9 µg/g_{TOC}; Jul.: 4.4 µg/g_{TOC}). The largest WWTP (Aachen-Soers) in the entire catchment area is located on this tributary.

Interestingly, in the more heavily polluted lower river, the cumulative concentrations of LABs in July were comparable and partly even lower than in the February samples. Perhaps, the volumes of wastewater (influents and effluents) were simply decreased in July, so that less LABs could be introduced to the Rur River. However, higher concentrations of LABs were detected in the upper reaches in July. In particular, a concentration increase was evident behind the Obermaubach reservoir (R5), where possibly an enrichment takes place due to altered flow characteristics. The overall increase in the contamination upstream could be due to additional flooding of smaller wastewater treatment plants in the Eifel area documented for the summer flood [9, 59]. Nonetheless, compared to the inputs in the more urbanized lower reaches, the relevance of the upper reaches to the total contamination is very low.

Depending on the position of the phenyl substitution, LABs can be distinguished in external substituted isomers (E) and internal substituted isomers (I). According to Takada and Ishiwatari [49] external substituted isomers are more readily biodegraded. Thus, the I/E ratio and therefore the changes of the isomer pattern of LABs can be used as indicator for the degree of microbial degradation. Ratios in untreated wastewater are typically close to 0.7, while higher values up to 7 represent ongoing microbial degradation [48]. For the Rur floodplains, the I/E ratios were between 0.4 and 2.3 in July and between 0.8 and 2.0 in February. This likely indicates a recent input of undegraded LABs from untreated sewage by the flood events, as these also inundated wastewater treatment plants along the river course [59]. In both campaigns, there is a very slight increase of I/E ratios from the upper to the lower reaches, possibly indicating initial degradation processes. Nevertheless, the values downstream were still comparable to those of barely treated sewage effluents.

In general, LABs have been introduced during both flood events. Thus, the dimension of the flood event does not seem to play a major role in their introduction, probably due to the direct spatial proximity of WWTPs and the receiving river. Therefore, an additional flood-induced LAB contamination should be regularly considered for any flood extent and dimension.

Compounds with enriched concentrations

After both flood events, PAHs occurred ubiquitously and mainly in high µg/g_{TOC} ranges (cf. Fig. 2). However, these contaminants generally show a diffuse emission, as there can be both petrogenic and pyrogenic sources. In the catchment area of the Rur river, lignite mining is a specific emission source of fossil matter derived contamination. However, in the case of natural disasters such as a flood, other input sources are also of key importance (e.g., stormwater runoff). Interestingly, in July the maximum EPA16 concentration of over 500 µg/g_{TOC} already occurred in the near-natural Eifel region (R2). There is a low settlement density and only limited industry. However, the sampling site is located directly on a so-called state road, which could be a pollution source due to its runoff. Elevated concentrations also appeared downstream of the Obermaubach reservoir (R5) and the Inde and Wurm tributaries (R10, R15). These two tributaries have themselves caused flooding and extreme damage along their courses, so they probably also discharged pollutants into the Rur [59]. The Obermaubach reservoir potentially collects pollutants from the upper reaches of the river because the flow velocity is highly reduced by the dam, allowing particulate material to settle and thus possibly be transported in higher concentrations during floods. According to Wolf et al. [61], there were also increased Cu- and Pb- concentrations at this location after the July flood highlighting the relevance of anthropogenic measures on the dispersion of different pollutants. At all three of the aforementioned sampling locations, the cumulative concentration of PAHs was above 300 µg/g_{TOC}. This is of high importance, because especially in the lower reaches, many areas adjacent to the river are used for agriculture.

In February, the maximum of nearly 250 µg/g_{TOC} occurred at a near-natural area close to Floßdorf (R12). In this area there is a nature reserve, which reflects the natural flow pattern of the Rur (wide meanders, almost unobstructed floodplains). Due to the reduced flow velocity, an increased flooding of the surrounding floodplains and thus the deposition of sedimentary material is very likely and thus explains the concentration peaks. Although the PAH concentration in Floßdorf was higher in July, the surrounding sampling locations also showed very high concentrations in summer, while in February the strong contamination occurred only locally. This again indicates a partial remobilization, but also additional emission sources in July. Similar high concentrations were detected in winter downstream of Abenden (R4: 247 µg/g_{TOC}) and thus, downstream of the Rurtalsperre. This reservoir also influences and changes the flow behavior, which may have led to sedimentation and relocation of the pollutants. However, the PAH sum at the corresponding sampling point decreased from February to July. Presumably, a remobilization of the contaminants took place there due to the considerable increase in the reservoir discharge of the Rurtalsperre caused by the flood. While the discharge in dry periods is about 5 m^3/s,

it was up to 41.5 m^3/s in January and even 97.7 m^3/s in July [58]. This large increase in discharge occurred within a short period of time and thus may have displaced sediments and soils, including accumulated pollutants, further downstream.

In July, benzo[b]fluoranthene, fluoranthene, pyrene and chrysene accounted for the largest contribution to the PAH pollution. Similarly, in February, fluoranthene, pyrene, phenanthrene and benzo[b]fluoranthene made up the largest shares. However, all of them suggest particularly a pyrogenic origin [3, 4, 44]. Further on, PAH diagnostic ratios were used to differentiate pollution emission sources such as combustion, petroleum or mixed sources. The ratios used in this study were anthracene and phenanthrene (An/(An + Ph)), benz[a]anthracene and chrysene (BaA/(BaA + Ch)), indeno[1,2,3-*cd*]pyrene and benzo[*g,h,i*]perylene (IP/(IP + Bghi)) plotted against the ratio of fluoranthene and pyrene (Fl/(Fl + Py)). Further on, C_1 phenanthrenes and anthracenes ($C_0/(C_0 + C_1)$ Ph + An) as well as C_1 fluoranthenes and pyrenes ratios ($C_0/(C_0 + C_1)$ Fl + Py) have been applied.

Most of the floodplain samples plot in the area of combustion, including petroleum combustion as well as grass, wood, or coal combustion (see Fig. 4). Pyrogenic emissions initially released into the air indicate a diffuse origin. According to Ahrens and Depree [2], asphalt pavements out of coal tar can also shift the compositional signature of PAHs towards a pyrogenic origin. Thus, PAHs could also have been introduced through damage to infrastructure and surface runoff. An exception to the identified pattern was the sampling point downstream of Düren (R8) in July, which plots in the mixed area of petroleum and combustion. Düren is the largest city and an urban as well as industrial agglomeration directly on the Rur River (~ 94,000 inhabitants). It is possible that petrogenic emissions from flooded industrial plants or urban areas were also introduced here. Generally, the scatter of points is larger for the samples of the summer flood indicating more and diverse emission sources.

Similar to PAHs and as shown in Fig. 2, geohopanes were also present in all samples. However, there were remarkable differences in concentrations depending on the different dimensions of the floods. The maximum cumulative concentration of C_{29}- to C_{35}-hopanes in July was 11.5 $\mu g/g_{TOC}$ and occurred at the Wurm tributary in the lower reaches (R15). Another considerable peak was caused by the Obermaubach reservoir (R5: 10.5 $\mu g/g_{TOC}$). As with PAHs, hopanes were probably retained and then released by the altered flow behavior (Obermaubach) or introduced by the damage caused at the tributary (Wurm). However, concentrations at the other sites also averaged more than 4 $\mu g/g_{TOC}$. This is more than ten times higher than the maximum hopane concentration in February, which was lower than 0.4 $\mu g/g_{TOC}$ and occurred at the head of the reservoir Rurtalsperre (R3). The lower reaches showed hardly any contamination in February indicating additional emission sources in summer. Thus, it cannot be clearly determined whether remobilization has taken place. Overall, the July flood resulted in remarkable petrogenic inputs due to industrial or urban flooding or the direct introduction of fossil fuels.

The maturity-dependent Ts/(Ts + Tm) ratio was nearly the same in both campaigns: between 0.23 and 0.49 in July and between 0.22 and 0.50 in February. This value is dependent both on maturity and source as it varies with organic matter inputs and source facies [11, 15, 32]. The ratios detected in this study are similar to those found in Middle East oils as well as some heavy oils from Venezuela, Canada and the USA [51, 56]. Typically, heavy oils are used for plastics, petrochemicals or road surfacing. Thus, the hopanes were probably introduced by remobilization and flooding of industrial or urban areas rather than fuels (as gasoline or diesel). Nevertheless, the Ts/(Ts + Tm) ratios indicate a petrogenic contamination with fossil material of enhanced maturity. The values were also similar to riverine samples from the Guilan province (Iran), which are also characterized by inputs of oil and its derivatives [43]. The ratio of 22S/(22S + 22R) C_{31}-hopanes ranged from 0.47 to 0.72 in July and from 0.45 to 1.00 in February. These ranges also point to enhanced maturities of fossil material with a predominance of 22*S* compared to the 22*R* epimer [22]. Possibly, petrogenic contamination took place as a consequence of flooding and destruction of, e.g., oil heating systems, industrial sites or vehicles. Again, similar results were obtained for riverine sediments in Iran highlighting the general distribution of fossil fuels in river systems [43].

However, PAH ratios are less indicative of relevant petrogenic contamination. Nevertheless, hopane concentrations and maturity parameters clearly show petrogenic inputs raising the question of the applicability of PAH and hopane markers in the field of environmental or flood pollution. According to Tobiszewski and Namieśnik [50], there are some limitations and PAH diagnostic ratios should be applied cautiously, as their values may change during the environmental fate of the corresponding substances. Some compounds are more sensitive to biodegradation, seasonal and other environmental changes, so that multiple authors recommend applying several diagnostic PAH ratios to confirm the results [5, 50, 63]. Low molecular weight PAHs in particular are less stable and should only be used with caution in diagnostic ratios [64]. Nonetheless, as shown in Fig. 4, all PAH cross plots showed mostly a pyrogenic contamination. However, PAHs from asphalt pavements also tend to indicate pyrolytic origins, although road surfaces are

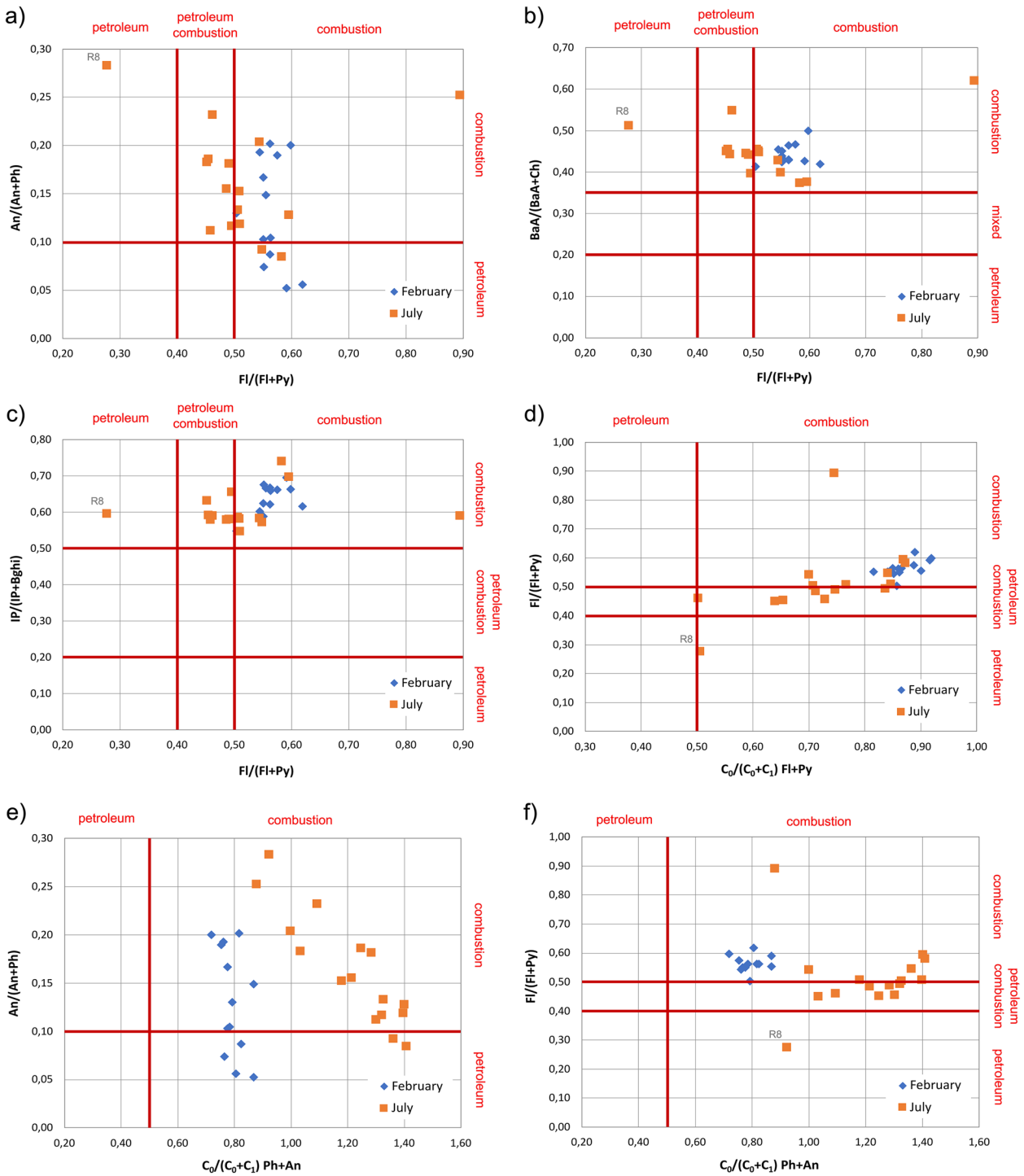

Fig. 4 PAH diagnostic ratios to differentiate and classify emission sources (petrogenic vs pyrogenic). Cross plots of **a** An/(An + Ph) vs. Fl/(Fl + Py), **b** BaA/(BaA + Ch) vs. Fl/(Fl + Py), **c** IP/(IP + Bghi) vs. Fl/(Fl + Py), **d** Fl/(Fl + Py) vs. $C_0/(C_0 + C_1)$ Fl + Py, **e** An/(An + Ph) vs. $C_0/(C_0 + C_1)$ Ph + An and **f** Fl/(Fl + Py) vs. $C_0/(C_0 + C_1)$ Ph + An according to Yunker et al. [63]

often made from heavy oils or bitumen and can accordingly be attributed to a petrogenic origin when considering hopane distribution. Generally, it must be taken into account that both pollutant groups are likely introduced from more than one source during flood events which cannot be clearly differentiated by diagnostic ratios. In

addition, concentrations of PAH contaminants were at least 20 times higher than hopane concentrations. Probably, contaminants of pyrogenic origin were just more present than petrogenic compounds, which, however, were clearly identified by hopanes and hopane maturity indicators. As a result of severe flooding, both (diffuse) pyrogenic and petrogenic contaminants are likely to be emitted into river systems. Therefore, different pollutant groups as well as different molecular ratios should always be considered and compared with the prevailing land use and industries.

PCBs are a very significant pollutant group to assess the remobilization potential of floods, because their use is now banned worldwide (in Germany since 1989). As with many other identified substances, the strongest pollution was present in the middle to lower course of the river with much higher concentrations in July. After the summer flood, the sampling location at Winden at the beginning of the Rur's middle course (R6) showed the cumulative maximum concentration of the representative congeners (PCB6) with almost 14 $\mu g/g_{TOC}$. Thus, the total PCB contamination at this location is estimated to be around 69 $\mu g/g_{TOC}$. The concentrations of the surrounding sampling points were very low, so this maximum is likely the result of a point source. One possible explanation is the flooding of the paper factory located at this site. As shown in Fig. 5, mainly high-chlorinated PCBs were detected (esp. Cl_6- and Cl_7-PCBs), which are more stable and resistant to degradation. However, the composition of PCBs also depends on the area of application and the decade of usage [16]. Higher chlorinated types were typically used as additives, e.g., in transformer oils, while low molecular weight products were frequently used in mining equipment [13, 37]. Thus, Cl_6- and Cl_7-PCBs at this site have been probably introduced by flooding of production sites and facilities or from contaminated sites in this industrial area.

In July, high cumulative PCB concentrations also occurred at Schophoven (R9), downstream of the Inde tributary (R10), and at Floßdorf (R12). Until 1944, the Inderevier was a former mining region for the extraction of hard coal [52]. It is possible that the July flood remobilized PCBs from corresponding mining sites and carried them into the Rur. The concentrations of low-chlorinated PCBs, which have often been used in underground mining processes, have also increased slightly (esp. Cl_3- and Cl_4-PCBs). They are 1.5 (Cl_3), respectively, nearly 2 times (Cl_4) as high as at the previous sampling location R9. However, these low-chlorinated congeners were not used for open-pit mining and since their usage is now generally banned, the current lignite mining at the Inde river does not seem to have an influence on PCB introduction. The sampling point at the nature reserve Floßdorf (R12) was remarkable in July as well as February 2021. In winter, it showed the maximum summed PCB6 concentration of 6.1 $\mu g/g_{TOC}$ (in July: 8.6 $\mu g/g_{TOC}$). The

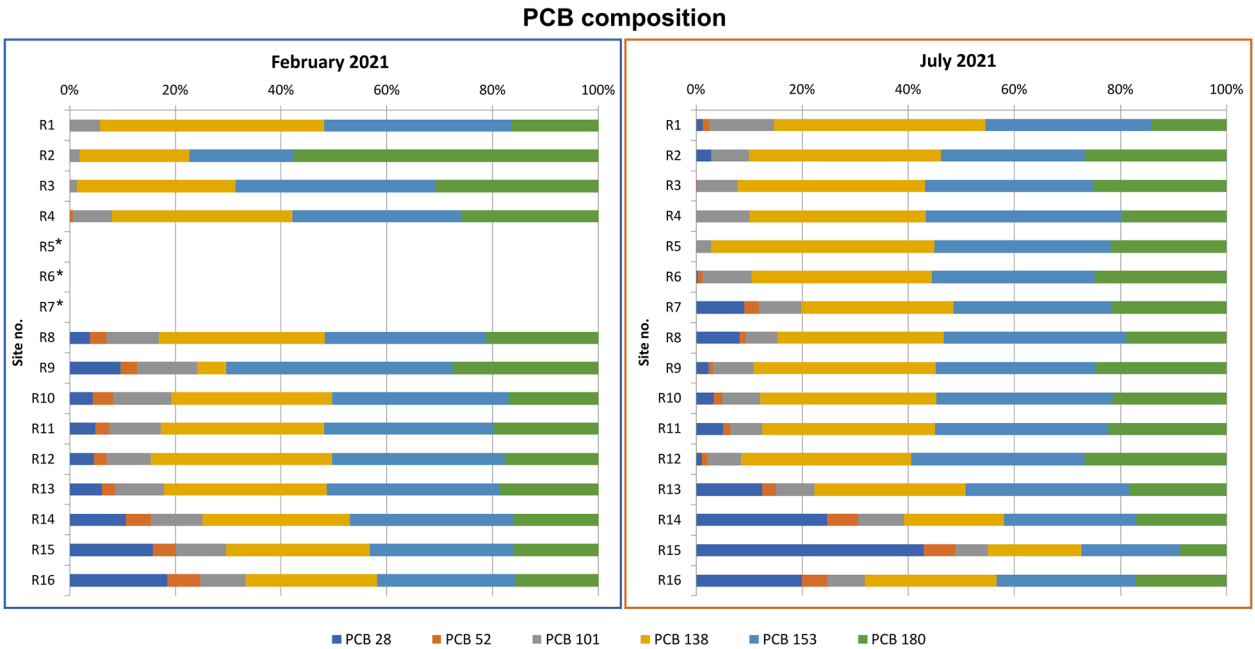

Fig. 5 Composition of the PCB mixtures divided into 6 representative congeners. Representative congeners are PCB 28, PCB 52, PCB 101, PCB 138, PCB 153, PCB 180. (*) R5 to R7 were not sampled in February

surrounding sampling locations had much lower concentrations that were almost the same in February and July, so remobilization processes in summer were probably not relevant. Instead, only an additional accumulation of pollutants in the floodplains at Floßdorf took place. Interestingly, concentrations at two monitoring sites were higher in February than in July. At Abenden (R4), downstream of the Rurtalsperre and downstream of Düren (R8), the concentrations were thus decreasing from February to July, possibly due to remobilization (e.g., by increased reservoir discharge).

Another remarkable feature regarding the PCB distribution pattern was that the proportions of higher-chlorinated PCBs decrease downstream and those of lower-chlorinated PCBs (esp. Cl_3-PCB 28) increase in July and slightly in February as well (see Fig. 5). Since the low-chlorinated PCBs show less environmental stability and have other typical applications (e.g., in mining), this indicates different emission sources than in the upper reaches. In July, high concentrations of the low-chlorinated PCB 28 were found after the Wurm tributary inflow (R15). In the Wurm catchment, underground mining of coal took place up to the end of the twentieth century, whereby the Wurm area was much more relevant than the aforementioned Inde region [52]. As the underground mining happened mainly at shallower depths, a flooding of respective sites and thus a remobilization of old mining burdens is quite likely [29]. However, there was probably no PCB input of these specific emission sources in February. Generally, the varying PCB proportions after the July flood indicate a more diverse input with additional and different emission sources.

As a last representative group of contaminants, the identified industrial additives generally showed higher concentrations in the lower reaches. The main contamination with DIPN occurred in the middle to lower reaches in both sampling campaigns. Again, the maximum value appeared in February at the natural river course near Floßdorf (R12: 4.1 $\mu g/g_{TOC}$). The maximum in July was further upstream next to a weir at Schophoven (R9: 14.2 $\mu g/g_{TOC}$). Emission sources are likely to be from the industrial sector around Düren, e.g., from flooding and damaging of corresponding facilities. The effect of the near-natural area of Floßdorf was no longer recognizable in July. Instead, there was a large concentration increase due to the Wurm tributary (R15: 10.0 $\mu g/g_{TOC}$) indicating damage to industrial areas or facilities on the Wurm itself. In February, the influence of the Rurtalsperre was also recognizable with an enriched accumulation of DIPN at the head of the reservoir (R3: 1.0 $\mu g/g_{TOC}$). The importance of such structural measures for pollutant distribution was also evident in July. Compared to the surrounding sampling locations, the site downstream of the Obermaubach reservoir showed increased concentrations of 2.6 $\mu g/g_{TOC}$ (R5).

Interestingly, the main contamination with Mesamoll® shifted upstream. In July, the highest concentrations (between 570 and 1300 ng/g_{TOC}) occurred downstream of the Rur and Obermaubach basins at R4 to R6 and at Schophoven (R9). Latter concentration peak could be a result of remobilization as the maximum concentration in February occurred at the previous location in the industrial center of Düren (R8: 750 ng/g_{TOC}). The second highest concentration in February was also attributed to urban settlement and the associated industry in Jülich (R11: 400 ng/g_{TOC}). However, locations R5 to R7 were not sampled in February, so a direct comparison of the maxima is difficult.

In July, DPE showed concentration peaks in Jülich (R11: 220 ng/g_{TOC}) and after the inflow of the Wurm tributary (R15: 800 ng/g_{TOC}). Jülich itself (34,000 inhabitants) is an industrial center for paper production, which is probably the main emission source of DPE in this river system. However, the paper industry is also important in the Düren area, where no considerably increased DPE concentrations occurred. In February, DPE was only found in the Eifel with much lower concentrations (max. 13 ng/g_{TOC}). As shown in Table 1, further (industrial) substances (e.g., butylated hydroxytoluene (BHT)) were also detected in July at higher concentrations and at more monitoring sites. While they were only detected sporadically or not at all in February, they were identified at most of the sites in July indicating additional emission sources from the industrial sector.

Influences of the river course, its structural adjustments as well as tributaries

As shown in Fig. 6, the sampling site near Floßdorf and the associated Rur meanders were particularly remarkable in connection with the winter flood, as the highest concentrations of many substances were detected there. In general, the Rur meanders influence the flow behavior and velocity, so that sedimentation of material occurs at the corresponding floodplains. In addition, this site is located downstream of the large urban and industrial areas of Jülich and Düren. The urban areas themselves did not show a high pollution. Possibly, the material and the pollutants emitted in those cities were transported to the floodplains at Floßdorf. Similar impacts on the river system were caused by weirs (as in Schophoven) or reservoirs (such as the Rurtalsperre or Obermaubach reservoir). They can function as a sink for sediments and sediment-bound pollutants, which are likely released during floods with high discharge. The latter illustrates the importance of structural anthropogenic measures in rivers for pollutant distribution and deposition.

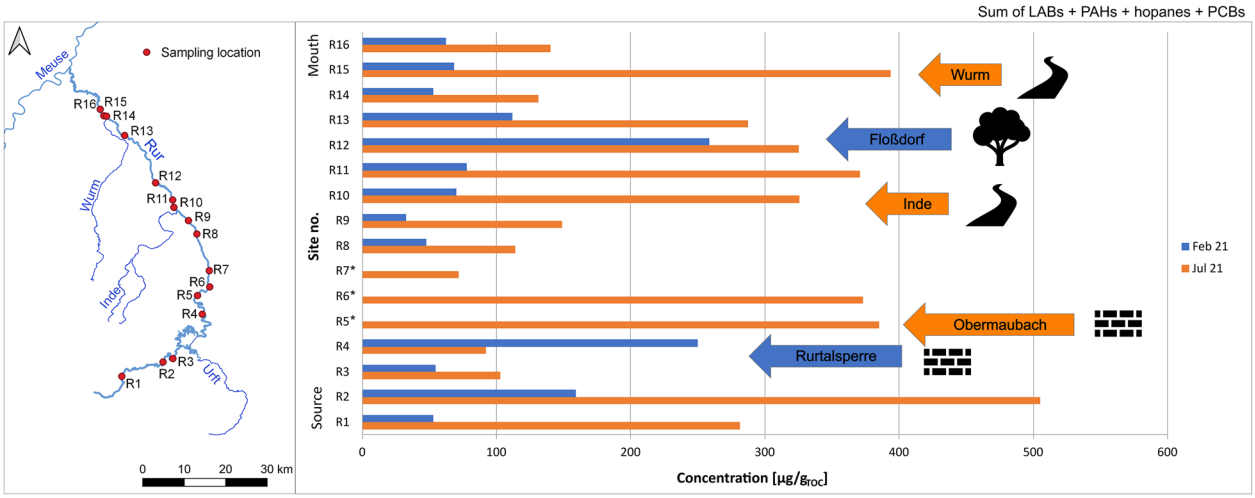

Fig. 6 Total contamination as a sum of LABs, PAHs, hopanes and PCBs in the Rur catchment. Samples have been taken after two flood events in January/February and July 2021. Important structural measures, (re)naturalized areas and tributaries are highlighted. (*) R5 to R7 were not sampled in February

Another clearly recognizable difference in the pollution situation occurred regarding the tributaries Inde and Wurm. In February, there were only very slight increases in concentrations, while in July there were large peaks for most of the identified substances. For instance, there was more than a doubling of the previous PAH concentrations. In July, both tributaries experienced severe flood damage, resulting in many pollutants being introduced into the rivers or remobilized and then transported. A considerable part was then also carried into the receiving river of the Rur and deposited there. Thus, both tributaries were major sources of contaminants in July 2021. The affected floodplains are located in the more agricultural part of the catchment system. This is of special relevance as it poses another (in)direct risk to humans.

However, flood protection also plays a decisive role in the mentioned influence of the tributaries. On the Inde and Wurm, flood protection measures are far less developed than on the Rur with its dam and reservoir system. For better understanding: the extreme inflows to the dam system from the catchment area of the Rur amounted to a total of approximately 760 m^3/s in July, but were retained in the Rur reservoirs and reduced to less than 100 m^3/s [57]. Consequently, the flood was less destructive in the lower course of the river. Nevertheless, such water retaining capacity was not present in the tributaries.

For most substances, the Wurm had a stronger impact on the pollution situation of the Rur river than the other tributaries. However, the flood caused worse destruction and damage on the Inde and its tributaries such as the Vichtbach [19, 47]. Thereby, a big part of the released and remobilized pollutants was probably deposited before they reached the course of the Rur. There are two explanations for this. In 2005, the last section of the Inde before its confluence with the Rur has been relocated and renaturalized due to the open-pit lignite mining in this region. Thus, the previously 5 km long old section was transformed into a 12.5 km long new course, whereby regular flooding of the adjacent floodplains was also taken into account [28]. Furthermore, during the summer flood in July 2021, the Inde river flooded and destroyed a dike near the open pit at the beginning of its relocation due to the high discharge, and a large part of the river water flowed into the lignite pit [35]. Accordingly, sedimentation of particulate matter as well as bound pollutants probably occurred in these areas, reducing the influence of the Inde river on the Rur River. Nevertheless, Inde and further tributaries were major emission sources, which underlines the need to investigate those areas for risk assessments where the pollutants are actually deposited. Hence, the relationship between micro- and meso-scale rivers should always be addressed during flood events.

Interestingly, regarding most of the pollutants the influences of the tributaries were only noticeable in July but caused peaks in LAB concentrations in both campaigns. There are many wastewater treatment plants located on the tributaries constantly discharging their effluents into the river system. Already the smaller, more regular winter flood caused the input of LABs in similar and, in the case of the Wurm tributary, even slightly higher concentrations than in July 2021. In general, the LAB input over the

entire river course was almost the same for both events and thus dimensions. Since LABs are an indicator of wastewater pollution, special attention should be given to these substances during flood events. Their introduction probably depends less on the dimension of the flood than on the occurrence of a flood itself. Even in the case of small events, a relevant input of substances from wastewater must be assumed. Possible reasons for the emission include the flooding of wastewater treatment basins, pumping stations or stormwater overflow basins, which are usually located a short distance from the rivers.

Conclusions

Accumulation of contaminated particulate matter in floodplains is of remarkable interest as it often results in a long-term storage. Thus, these sediment deposits can act as ecological archives, but also as secondary emission sources due to remobilization processes during large flood events. Therefore, it is of particular importance to consider the pollution at those rivers and its floodplains where the contaminants are actually deposited. In the catchment area of the Rur, especially in July 2021, major damage occurred to infrastructure, industry, agricultural and urban areas, particularly on the tributaries Wurm and Inde. However, many of the released pollutants were then deposited in the floodplains of the superior Rur river. This shows the large impact of smaller rivers on meso-scaled catchment systems and the relevance of remobilization for risk assessments. On the Rur itself, there are already several flood protection measures in place, and the dams and reservoirs have reduced discharges of the summer flood to a manageable level. However, such measures did not exist at the tributaries of the Rur. This statement is also true for many other micro-scale rivers in Germany and Europe. Therefore, meso-scaled river systems are particularly important for short- and long-term risk assessments since many of the pollutants accumulate and remain in their floodplains. Nevertheless, the accumulation and distribution processes are also highly influenced by structural measures, which must be carefully considered (e.g., an enrichment of pollutants in dam sediments that may be released during floods). In this context, different pollutants and pollutant groups may also exhibit different behavioral patterns (as identified here for LABs). Overall, organic indicators are very useful to gain information about indirect flood effects and the relevance of morphological settings. Especially regarding climate change and the increasing tendency of heavy rainfall and flood events, these factors need to be addressed as it was done in this study using the example of the meso-scaled Rur catchment.

Abbreviations

BHT	Butylated hydroxytoluene
DCM	Dichloromethane
DIPNs	Di-*iso*-propylnaphthalenes
DPE	1,2-Diphenoxyethane
GC/MS	Gas chromatography/mass spectrometry
LABs	Linear alkylbenzenes
LOI	Loss on ignition
PAHs	Polycyclic aromatic hydrocarbons
PCBs	Polychlorinated biphenyls
POPs	Persistent organic pollutants
TC	Total carbon
TIC	Total inorganic carbon
TOC	Total organic carbon
WWTP	Wastewater treatment plant

Supplementary Information

The online version contains supplementary material available at https://doi.org/10.1186/s12302-023-00717-4.

Additional file 1: Additional figures and tables.

Acknowledgements

Special thanks to the support of Mrs. Yvonne Esser and Mrs. Annette Schneiderwind during laboratory work. In addition, CS thanks the RWTH Scholarships for Doctoral Students.

Author contributions

CS wrote the first draft of the manuscript. All authors contributed to specific aspects of the manuscript. All authors read and approved the final manuscript.

Funding

Open Access funding enabled and organized by Projekt DEAL. CS was financially supported by the RWTH Aachen University Scholarships for Doctoral Students.

Availability of data and materials

All data generated or analyzed during this study are included in this published article and its Additional file 1.

Declarations

Ethics approval and consent to participate

Not applicable.

Consent for publication

Not applicable.

Competing interests

The authors declare that they have no competing interests.

Received: 22 December 2022 Accepted: 22 January 2023
Published online: 06 March 2023

References

1. Abdel-Shafy HI, Mansour MS (2016) A review on polycyclic aromatic hydrocarbons: source, environmental impact, effect on human health and remediation. Egypt J Pet 25:107–123. https://doi.org/10.1016/j.ejpe.2015.03.011
2. Ahrens MJ, Depree CV (2010) A source mixing model to apportion PAHs from coal tar and asphalt binders in street pavements and urban aquatic sediments. Chemosphere 81:1526–1535. https://doi.org/10.1016/j.chemosphere.2010.08.030

3. Akpambang V, Akpoesiri I (2016) Levels and sources of polycyclic aromatic hydrocarbons in urban soils of Akure, Nigeria. Chem Sci Int J. https://doi.org/10.9734/CSJI/2016/30108
4. Bellanova P, Frenken M, Richmond B, Schwarzbauer J, La Selle S, Griswold F, Jaffe B, Nelson A, Reicherter K (2020) Organic geochemical investigation of far-field tsunami deposits of the Kahana Valley, O'ahu, Hawai'i. Sedimentology 67:1230–1248. https://doi.org/10.1111/sed.12583
5. Biache C, Mansuy-Huault L, Faure P (2014) Impact of oxidation and biodegradation on the most commonly used polycyclic aromatic hydrocarbon (PAH) diagnostic ratios: Implications for the source identifications. J Hazard Mater 267:31–39. https://doi.org/10.1016/j.jhazmat.2013.12.036
6. BMI (2021) Bericht zur Hochwasserkatastrophe 2021: Katastrophenhilfe, Wiederaufbau und Evaluierungsprozesse. Bundesministerium des Innern und für Heimat Bundesministerium der Finanzen, Berlin
7. Boccacco Mariani M, Chiacchierini E, Gesumundo C (1999) Potential migration of diisopropyl naphthalenes from recycled paperboard packaging into dry foods. Food Addit Contam 16:207–213. https://doi.org/10.1080/026520399284073
8. Crawford SE, Brinkmann M, Ouellet JD, Lehmkuhl F, Reicherter K, Schwarzbauer J, Bellanova P, Letmathe P, Blank LM, Weber R, Brack W, van Dongen JT, Menzel L, Hecker M, Schüttrumpf H, Hollert H (2022) Remobilization of pollutants during extreme flood events poses severe risks to human and environmental health. J Hazard Mater 421:126691. https://doi.org/10.1016/j.jhazmat.2021.126691
9. Eifeler Presse Agentur (2021) Auch Kläranlagen des WVER vom Hochwasser betroffen. https://eifeler-presse-agentur.de/2021/07/20/auch-klaeranlagen-des-wver-vom-hochwasser-betroffen/. Accessed 30 Aug 2022
10. ELWAS-WEB (2022) Information about the gauging station Jülich. http://www.elwas.web.nrw.de. Accessed 23 Sep 2022
11. Farrimond P, Taylor A, TelnÆs N (1998) Biomarker maturity parameters: the role of generation and thermal degradation. Org Geochem 29:1181–1197. https://doi.org/10.1016/S0146-6380(98)00079-5
12. Franke S, Grunenberg J, Schwarzbauer J (2007) The isomer-specific analysis of di- iso-propylnaphthalenes. Int J Environ Anal Chem 87:437–448. https://doi.org/10.1080/03067310601025221
13. Friege H, Stock W, Alberti J, Poppe A, Juhnke I, Knie J, Schiller W (1989) Environmental behaviour of polychlorinated monomethyl-substituted diphenyl-methanes (Me-PCDMs) in comparison with polychlorinated biphenyls (PCBs) II: environmental residues and aquatic toxicity. Chemosphere 18:1367–1378. https://doi.org/10.1016/0045-6535(89)90028-3
14. Fromme H, Schwarzbauer J, Lahrz T, Kraft M, Fembacher L (2017) Alkylsulfonic acid phenylesters (ASEs, Mesamoll®) in dust samples of German residences and daycare centers (LUPE 3). Int J Hyg Environ Health 220:440–444. https://doi.org/10.1016/j.ijheh.2016.12.009
15. Gao X, Chen S, Xie X, Long A, Ma F (2007) Non-aromatic hydrocarbons in surface sediments near the Pearl River estuary in the South China Sea. Environ Pollut 148:40–47. https://doi.org/10.1016/j.envpol.2006.11.001
16. Hagemann L, Buchty-Lemke M, Lehmkuhl F, Alzer J, Kümmerle EA, Schwarzbauer J (2018) Exhaustive screening of long-term pollutants in riverbank sediments of the Wurm River, Germany. Water Air Soil Pollut. https://doi.org/10.1007/s11270-018-3843-9
17. Haritash AK, Kaushik CP (2009) Biodegradation aspects of polycyclic aromatic hydrocarbons (PAHs): a review. J Hazard Mater 169:1–15. https://doi.org/10.1016/j.jhazmat.2009.03.137
18. Heim S, Schwarzbauer J, Kronimus A, Littke R, Woda C, Mangini A (2004) Geochronology of anthropogenic pollutants in riparian wetland sediments of the Lippe River (Germany). Org Geochem 35:1409–1425. https://doi.org/10.1016/j.orggeochem.2004.03.008
19. Hermanns H (2021) Millionenschäden durch das Hochwasser im Raum Aachen. https://www1.wdr.de/nachrichten/rheinland/millionen-schaeden-hochwasser-100.html. Accessed 28 Apr 2022
20. Hirabayashi Y, Mahendran R, Koirala S, Konoshima L, Yamazaki D, Watanabe S, Kim H, Kanae S (2013) Global flood risk under climate change. Nat Clim Chang 3:816–821. https://doi.org/10.1038/NCLIMATE1911
21. Ionita M, Scholz P, Grosfeld K (2021) July heavy rains and floods in western part of Germany: evolution of a tragedy!. https://www.reklim.de/en/archive-news/news-2021/july-heavy-rains-and-floods-in-western-germany/. Accessed 25 Apr 2022
22. Jeanneau L, Faure P, Montarges-Pelletier E, Ramelli M (2006) Impact of a highly contaminated river on a more important hydrologic system: changes in organic markers. Sci Total Environ 372:183–192. https://doi.org/10.1016/j.scitotenv.2006.09.021
23. Klös H, Schoch C (1993) Historische Entwicklung einer Sedimentbelastung: Gedächtnis einer Industrieregion. Acta hydrochim hydrobiol 21:32–37. https://doi.org/10.1002/aheh.19930210105
24. Koenzen U, Kurth A, Günther-Diringer D (2021) Auenzustandsbericht 2021: Flussauen in Deutschland. Bundesministerium für Umwelt, Naturschutz und nukleare Sicherheit, Bundesamt für Naturschutz, Bonn
25. Kreienkamp F, Philip SY, Tradowsky JS, Kew SF, Lorenz P, Arrighi J, Belleflamme A, Bettmann T, Caluwaerts S, Chan SC, Ciavarella A, De Cruz L, de Vries H, Demuth N, Ferrone A, Fischer EM, Fowler HJ, Goergen K, Heinrich D, Henrichs Y, Lenderink G, Kaspar F, Nilson E, Otto FE, Ragone F, Seneviratne SI, Singh RK, Skalevag A, Termonia P, Thalheimer L, van Aalst M, Van den Bergh J, Van de Vyver H, Vannitsem S, van Oldenborgh GJ, Van Schaeybroeck B, Vautard R, Vonk D, Wanders N (2021) Rapid attribution of heavy rainfall events leading to the severe flooding in Western Europe during July 2021. World Weather Attribution. https://www.worldweatherattribution.org/wp-content/uploads/Scientific-report-Western-Europe-floods-2021-attribution.pdf. Accessed 1 Feb 2023
26. Kundzewicz ZW, Pińskwar I, Brakenridge GR (2013) Large floods in Europe, 1985–2009. Hydrol Sci J 58:1–7. https://doi.org/10.1080/02626667.2012.745082
27. León VM, Moreno-González R, García V, Campillo JA (2017) Impact of flash flood events on the distribution of organic pollutants in surface sediments from a Mediterranean coastal lagoon (Mar Menor, SE Spain). Environ Sci Pollut Res 24:4284–4300. https://doi.org/10.1007/s11356-015-4628-y
28. Maaß A-L, Esser V, Frings RM, Lehmkuhl F, Schüttrumpf H (2018) A decade of fluvial morphodynamics: relocation and restoration of the Inde River (North-Rhine Westphalia, Germany). Environ Sci Eur 30:40. https://doi.org/10.1186/s12302-018-0170-0
29. Maaß A-L, Schüttrumpf H (2018) Long-term effects of mining-induced subsidence on the trapping efficiency of floodplains. Anthropocene 24:1–13. https://doi.org/10.1016/j.ancene.2018.10.001
30. Maliszewska-Kordybach B, Klimkowicz-Pawlas A, Smreczak B, Gałązka R (2012) Effect of flooding on contamination of agricultural soils with metals and PAHs: the middle Vistula gap case study. Water Air Soil Pollut 223:687–697. https://doi.org/10.1007/s11270-011-0894-6
31. Martínez-Santos M, Probst A, García-García J, Ruiz-Romera E (2015) Influence of anthropogenic inputs and a high-magnitude flood event on metal contamination pattern in surface bottom sediments from the Deba River urban catchment. Sci Total Environ 514:10–25. https://doi.org/10.1016/j.scitotenv.2015.01.078
32. Peters KE, Walters CC, Moldowan JM (2007) Biomarker guide: volume 2, biomarkers and isotopes in petroleum systems and Earth history. Cambridge University Press, Cambridge
33. Pye K, Blott SJ (2004) Particle size analysis of sediments, soils and related particulate materials for forensic purposes using laser granulometry. Forensic Sci Int 144:19–27. https://doi.org/10.1016/j.forsciint.2004.02.028
34. Raynaud D, Thielen J, Salamon P, Burek P, Anquetin S, Alfieri L (2015) A dynamic runoff co-efficient to improve flash flood early warning in Europe: evaluation on the 2013 central European floods in Germany. Meteorol Appl 22:410–418. https://doi.org/10.1002/met.1469
35. RWE AG (2021) RWE-Kraftwerke von der Hochwasserkatastrophe betroffen. https://www.rwe.com/presse/rwe-ag/2021-07-17-rwe-kraftwerke-von-der-hochwasserkatastrophe-betroffen. Accessed 28 Apr 2022
36. Schäfer A, Mühr B, Daniell J, Ehret U, Ehmele F, Küpfer K, Brand J, Wisotzky C, Skapski J, Rentz L, Mohr S, Kunz M (2021) Hochwasser Mitteleuropa, Juli 2021 (Deutschland): 21. Juli 2021 – Bericht Nr. 1"Nordrhein-Westfalen and Rheinland-Pfalz". CEDIM, Karlsruhe
37. Schettgen T, Alt A, Schikowsky C, Esser A, Kraus T (2018) Human biomonitoring of polychlorinated biphenyls (PCBs) in plasma of former underground miners in Germany - a case-control study. Int J Hyg Environ Health 221:1007–1011. https://doi.org/10.1016/j.ijheh.2018.06.006
38. Schulte P, Lehmkuhl F (2018) The difference of two laser diffraction patterns as an indicator for post-depositional grain size reduction in loess-paleosol sequences. Palaeogeogr Palaeoclimatol Palaeoecol 509:126–136. https://doi.org/10.1016/j.palaeo.2017.02.022
39. Schulte P, Lehmkuhl F, Steininger F, Loibl D, Lockot G, Protze J, Fischer P, Stauch G (2016) Influence of HCl pretreatment and organo-mineral

complexes on laser diffraction measurement of loess–paleosol-sequences. CATENA 137:392–405. https://doi.org/10.1016/j.catena.2015.10.015
40. Schwanen CA, Schwarzbauer J (2022) Structural diversity of organic contaminants in a meso-scaled river system. Water Air Soil Pollut. https://doi.org/10.1007/s11270-022-05503-1
41. Schwarzbauer J, Jovančićević B (2018) Organic pollutants in the geosphere. Springer International Publishing, Cham
42. Schwarzbauer J, Littke R, Weigelt V (2000) Identification of specific organic contaminants for estimating the contribution of the Elbe river to the pollution of the German Bight. Org Geochem 31:1713–1731. https://doi.org/10.1016/S0146-6380(00)00076-0
43. Shirneshan G, Bakhtiari AR, Memariani M (2016) Distribution and origins of n-alkanes, hopanes, and steranes in rivers and marine sediments from Southwest Caspian coast, Iran: implications for identifying petroleum hydrocarbon inputs. Environ Sci Pollut Res 23:17484–17495. https://doi.org/10.1007/s11356-016-6825-8
44. Sicre M-A, Fernandes MB, Pont D (2008) Poly-aromatic hydrocarbon (PAH) inputs from the Rhône River to the Mediterranean Sea in relation with the hydrological cycle: impact of floods. Mar Pollut Bull 56:1935–1942. https://doi.org/10.1016/j.marpolbul.2008.07.015
45. Stadt Jülich (2021) Hochwasserkatastrophe 14. - 16.07.2021 in Jülich. https://www.juelich.de/hochwasserkarten. Accessed 28 Apr 2022
46. Aachen StUA (2005) Ergebnisbericht Rur und südliche sonstige Maaszuflüsse: Bearbeitungsgebiet Maas-Deutschland (Süd). Wasserrahmenrichtlinie in NRW, Bestandsaufnahme. Ministerium für Umwelt und Naturschutz, Landwirtschaft und Verbraucherschutz des Landes Nordrhein-Westfalen, Düsseldorf
47. Szönyi M, Roezer V, Deubelli T, Ulrich J, MacClune K, Laurien F, Norton R (2022) PERC floods following "Bernd." Zurich Insurance Company, Zurich
48. Takada H, Eganhouse RP (1998) Molecular markers of anthropogenic waste. In: Meyers RA (ed) Encyclopedia of environmental analysis and remediation. Wiley, New York
49. Takada H, Ishiwatari R (1990) Biodegradation experiments of linear alkylbenzenes (LABs): isomeric composition of C12 LABs as an indicator of the degree of LAB degradation in the aquatic environment. Environ Sci Technol 24:86–91. https://doi.org/10.1021/es00071a009
50. Tobiszewski M, Namieśnik J (2012) PAH diagnostic ratios for the identification of pollution emission sources. Environ Pollut 162:110–119. https://doi.org/10.1016/j.envpol.2011.10.025
51. Volkman JK, Revill AT, Murray AP (1997) Applications of biomarkers for identifying sources of natural and pollutant hydrocarbons in aquatic environments. In: Eganhouse RP (ed) Molecular markers in environmental geochemistry. American Chemical Society, Washington DC
52. Voncken J (2020) Geology of coal deposits of South Limburg, the Netherlands. Springer International Publishing, Cham
53. Vulava VM, Vaughn DS, McKay LD, Driese SG, Cooper LW, Menn F-M, Levine NS, Sayler GS (2017) Flood-induced transport of PAHs from streambed coal tar deposits. Sci Total Environ 575:247–257. https://doi.org/10.1016/j.scitotenv.2016.09.222
54. Waid JS (1986) PCBs and the environment. CRC Press, Boca Raton
55. Walker DB, Baumgartner DJ, Gerba CP, Fitzsimmons K (2019) Surface water pollution. In: Brusseau ML, Pepper IL, Gerba CP (eds) Environmental and Pollution Science. Elsevier, London
56. Wang Z, Fingas M, Yang C, Christensen JH (2005) Crude oil and refined product fingerprinting: principles. In: Morrison RD, Murphy BL (eds) Environmental forensics: contaminant specific guide. Elsevier, Amsterdam
57. Wasserverband Eifel-Rur (2021) Extremes Hochwasser 2021—Bürgerinformation. https://wver.de/buergerinformation-hochwasser-2021/. Accessed 8 Nov 2022
58. Wasserverband Eifel-Rur (2021) Verfügbare Messstellen und Zeitreihen, aktuelle Werte (MEZ). https://server.wver.de/pegeldaten/. Accessed 26 Jul 2021
59. Wasserverband Eifel-Rur (2021) WVER-Eilmeldung zur Hochwassersituation an der Rur, 19.07.2021, 21:00 Uhr. https://wver.de/wver-eilmeldung-zur-hochwassersituation-an-der-rur-15-07-2021-1830-uhr/. Accessed 25 Apr 2022
60. Wilby RL, Keenan R (2012) Adapting to flood risk under climate change. Prog Phys Geogr 36:348–378. https://doi.org/10.1177/0309133312438908
61. Wolf S, Esser V, Lehmkuhl F, Schüttrumpf H (2022) Long-time impact of a large dam on its downstream river's morphology: determined by sediment characteristics, pollutants as a marker, and numerical modelling. J Sediment Environ 7:403–424. https://doi.org/10.1007/s43217-022-00103-9
62. Yunker MB, Macdonald RW (2003) Petroleum biomarker sources in suspended particulate matter and sediments from the Fraser River Basin and Strait of Georgia, Canada. Org Geochem 34:1525–1541. https://doi.org/10.1016/S0146-6380(03)00157-8
63. Yunker MB, Macdonald RW, Vingarzan R, Mitchell RH, Goyette D, Sylvestre S (2002) PAHs in the Fraser River basin: a critical appraisal of PAH ratios as indicators of PAH source and composition. Org Geochem 33:489–515. https://doi.org/10.1016/S0146-6380(02)00002-5
64. Zhang XL, Tao S, Liu WX, Yang Y, Zuo Q, Liu SZ (2005) Source diagnostics of polycyclic aromatic hydrocarbons based on species ratios: a multimedia approach. Environ Sci Technol 39:9109–9114. https://doi.org/10.1021/es0513741

Publisher's Note